

Orthogonal Control of Gene Expression in Plants Using Synthetic Promoters and CRISPR-Based Transcription Factors

Shaunak Kar (✉ shaunak@utexas.edu)

The University of Texas at Austin <https://orcid.org/0000-0003-3354-1789>

Yogendra Bordiya

The University of Texas at Austin

Nestor Rodriguez

The University of Texas at Austin

Junghyun Kim

The University of Texas at Austin

Elizabeth C Gardner

The University of Texas at Austin

Jimmy D Gollihar

US Army Research Laboratory

Sibum Sung

The University of Texas at Austin

Andrew D Ellington

The University of Texas at Austin

Research Article

Keywords: Synthetic transcription factor, orthogonal promoter, modular cloning, plant synthetic biology

Posted Date: January 3rd, 2022

DOI: <https://doi.org/10.21203/rs.3.rs-1194009/v1>

License: © ⓘ This work is licensed under a Creative Commons Attribution 4.0 International License.

[Read Full License](#)

1 **Orthogonal control of gene expression in plants using synthetic**
2 **promoters and CRISPR-based transcription factors**

3
4 Shaunak Kar^{1,2,#,*}, Yogendra Bordiya^{1,4,#}, Nestor Rodriguez¹, Junghyun Kim¹, Elizabeth
5 C. Gardner^{1,2}, Jimmy D. Gollihar³, Sibum Sung^{1,*} and Andrew D. Ellington^{1,2,*}
6
7

8 ¹ Department of Molecular Biosciences, University of Texas at Austin, Austin TX, USA

9 ² Center for Systems and Synthetic Biology, University of Texas at Austin, Austin, TX,
10 USA

11 ³ US Army Research Laboratories–South, Austin, Texas, USA

12 ⁴ Present address: Life Sciences Solutions group, Thermo Fisher Scientific, Austin, TX,
13 USA

14
15 # Authors contributed equally

16 * Corresponding authors
17

18 Shaunak Kar: shaunak@utexas.edu

19 Sibum Sung: sbsung@austin.utexas.edu

20 Andrew D. Ellington: ellingtonlab@gmail.com
21
22

23 **Abstract**
24

25 **Background:** The construction and application of synthetic genetic circuits is frequently
26 improved if gene expression can be orthogonally controlled, relative to the host. In plants,
27 orthogonality can be achieved via the use of CRISPR-based transcription factors that are
28 programmed to act on natural or synthetic promoters. The construction of complex gene
29 circuits can require multiple, orthogonal regulatory interactions, and this in turn requires
30 that the full programmability of CRISPR elements be adapted to non-natural and non-
31 standard promoters that have few constraints on their design. Therefore, we have
32 developed synthetic promoter elements in which regions upstream of the minimal 35S

33 CaMV promoter are designed from scratch to interact via programmed gRNAs with dCas9
34 fusions that allow activation of gene expression.

35

36 **Results:** A panel of three, mutually orthogonal promoters that can be acted on by artificial
37 gRNAs bound by CRISPR regulators were designed. Guide RNA expression targeting
38 these promoters was in turn controlled by either Pol III (U6) or ethylene-inducible Pol II
39 promoters, implementing for the first time a fully artificial Orthogonal Control System
40 (OCS). Following demonstration of the complete orthogonality of the designs, the OCS
41 was tied to cellular metabolism by putting gRNA expression under the control of an
42 endogenous plant signaling molecule, ethylene. The ability to form complex circuitry was
43 demonstrated via the ethylene-driven, ratiometric expression of fluorescent proteins in
44 single plants.

45

46 **Conclusions:** The design of synthetic promoters is highly generalizable to large tracts
47 of sequence space, allowing Orthogonal Control Systems of increasing complexity to
48 potentially be generated at will. The ability to tie in several different basal features of
49 plant molecular biology (Pol II and Pol III promoters, ethylene regulation) to the OCS
50 demonstrates multiple opportunities for engineering at the system level. Moreover, given
51 the fungibility of the core 35S CaMV promoter elements, the derived synthetic promoters
52 can potentially be utilized across a variety of plant species.

53

54

55 **Keywords**

56 Synthetic transcription factor, orthogonal promoter, modular cloning, plant synthetic
57 biology

58

59 **Introduction**

60

61 The field of synthetic biology aims to revolutionize biotechnology by rationally engineering
62 living organisms (1-6). One aspect of rational engineering is to embed biological
63 organisms with complex information processing systems that can be used to control
64 phenotypes (2, 3, 7, 8), often via synthetic gene circuits that can predictably regulate
65 and tune expression of endogenous as well as transgenes (4, 9-11).

66 However the performance of such synthetic genetic circuits is often plagued by unwanted
67 interactions between the circuit components and the host regulatory system, which can
68 lead to loss of circuit function (10). These unprogrammed interactions can be mitigated
69 via the design and use of genetic parts that have minimal cross-talk with the host, creating
70 orthogonal regulatory or orthogonal control systems (OCS) that can further serve as the
71 basis for constructing complex genetic programs with predictable behaviors. In the last
72 two decades an increasing number of well-characterized genetic parts have been
73 combined in circuits capable of complex dynamic behaviors, including bi-stable switches,
74 oscillators, pulse generators, Boolean-complete logic gates (7, 12-15). While OCS and
75 the circuits that comprise them were initially characterized in microbial hosts, more
76 recently a significant fraction of them have been constructed and characterized in

77 eukaryotic hosts such as yeast and mammalian cells (12, 16-19). More recently, synthetic
78 transcriptional control elements have begun to be characterized in plants (20-22).

79 While a variety of artificial plant transcription factors containing diverse DNA binding
80 domains and plant-specific regulatory sequences are known (20, 22), orthogonal control
81 requires more programmable DNA binding domains and modular regulatory domains (20,
82 22-24). To this end, we describe an alternate strategy for the construction of orthogonal
83 transcriptional regulatory elements in plants, powered by a single universal transcriptional
84 factor – dCas9:VP64 which has been shown to work in a wide variety of eukaryotic
85 species, including plants (16, 25, 26). While this transcription factor has primarily been
86 used for the regulation of endogenous genes (25-27), here we describe a generalizable
87 strategy for the universal design and use of synthetic promoters that rely only on the
88 production of specific gRNAs to program dCas9:VP64, and the use of this set of mutually
89 orthogonal promoters for the bottom-up construction of circuits that show multiplexed
90 control of gene expression.

91

92 **Results**

93 **Design of a modular cloning framework for facile construct assembly**

94

95 Traditionally the process of construction of these synthetic gene expression systems has
96 relied on time-consuming practices of recombinant DNA technology like design of custom
97 primers, PCR amplification, gel extraction of PCR products. Over the last decade the
98 advent of high-throughput cloning techniques, such as Golden-gate cloning with Type IIS

99 restriction enzymes, has greatly accelerated the design-build-test cycle for the
100 construction and prototyping of synthetic circuits (7, 9, 28, 29). Because the overlaps for
101 assemblies can be modularly specified, multiple parts can be assembled sequentially in
102 a single tube reaction.

103 While a Golden-Gate framework was previously described for the construction of plant
104 expression vectors (30), here we used the highly optimized modular cloning (MoClo)
105 framework, instantiated as a yeast toolkit (YTK) as the basis of our architecture (28).
106 Recently, beyond yeast expression vectors, this framework has been adapted for the
107 construction of a mammalian toolkit (MTK) (9). Along with both YTK and MTK, a plant
108 toolkit based on the YTK architecture will prove essential for seamlessly porting parts and
109 circuits across diverse eukaryotes. Briefly, in this framework the entire vector is divided
110 into particular ‘part’ types flanked by BsaI restriction sites followed by a unique ligation
111 site. Promoters, genes and terminators are generally categorized into Type 2, 3 and 4
112 parts respectively where each part type has a unique overhang that dictates the
113 compatibility between part types (9, 28) (**Fig 1A, S1A**). This preserves the architecture of
114 each transcriptional unit (promoter-gene-terminator). For the assembly of multiple
115 transcriptional units (TU), each transcriptional unit is first cloned into an ‘intermediate’
116 vector flanked by connector sequences that dictate the order of the TUs to be stitched
117 together. By using appropriate connectors, each TU can be further assembled into a final
118 expression vector in a single pot reaction (**Fig S1B**) [20]. This modular approach enables
119 rapid assembly of increasingly complex genetic circuits comprised of multiple
120 transcriptional units.

121 Since *Agrobacterium*-based transformation has been the staple for plant genetic
122 engineering for decades (31), we used compatible vectors as the basis for our framework,
123 and designed and constructed three YTK-compatible shuttle vectors. Each expression
124 vector contains the pVS1 replicon (an *Agrobacterium* origin of replication – OriV and two
125 supporting proteins – RepA and StaA) and pBR22 origin for propagation in *Agrobacterium*
126 and *E.coli* respectively, and a common antibiotic selection cassette (KanR) that has been
127 shown to be functional in both species (**Fig 1B, Materials and Methods**) (29, 30). The
128 three constructs otherwise differed in the plant selection marker - BASTA, hygromycin,
129 and kanamycin. The resistance markers were expressed from the Nos promoter and also
130 contained a Nos terminator (30) (**Fig 1B**). The backbone also contains a GFP drop-out
131 cassette that allows easy identification of correct assemblies, which should appear as
132 colonies that lack fluorescence (9, 28) (**Fig 1B**).

133

134 Fluorescence and luminescence reporters are frequently used to study protein
135 localization and interaction in plants and animals (32). To provide these useful reporter
136 parts in the context of our system, we cloned the strong promoter from Cauliflower mosaic
137 virus (35S) as a Type 2 part and its corresponding terminator as a Type 4 part (33, 34).
138 These parts can be matched with a number of fluorescent reporter genes (GFP, BFP,
139 YFP and RFP) all as Type 3 parts for robust reporter expression. Combinations of these
140 proteins can also potentially be used for BIFC (Bimolecular Fluorescence
141 Complementation) (35). Similarly, luciferase is commonly used in plant molecular biology
142 to study circadian rhythm (36), test the spatiotemporal activities of regulatory elements

143 (37), and to study the plant immune system (38, 39). Therefore we adapted a luciferase
144 gene from *Photinus pyralis*, commonly known as firefly luciferase (F-luc) (21).

145
146 Single TUs comprised of a 35S promoter, fluorescent reporter genes and the luciferase
147 gene, and a terminator that serves as a polyadenylation signal were assembled into the
148 *Agrobacterium* shuttle expression vector (**Fig 2A-C**). The activity of constructs was
149 assayed using transient expression in *Nicotiana benthamiana* (30). As expected, we see
150 strong activity of the promoter with the expression of the respective reporter genes (**Fig**
151 **2A-C**). In order to diversify the promoters used in circuits (and thereby avoid
152 recombination and potentially silencing), we also included a well-characterized promoter
153 from the Ti plasmid that drives mannopine synthase (Pmas) (40-43). When the 35S
154 promoter was swapped with Pmas, similar expression levels of YFP were achieved (**Fig**
155 **2D**).

156

157 **Development of an Orthogonal Control System (OCS) to regulate transgene** 158 **expression**

159 One of the primary difficulties with using synthetic biology principles and methods to
160 engineer organisms, especially in eukaryotes, is that the functionality of synthetic circuits
161 is often plagued by unwanted interactions of the circuit 'parts' with the underlying
162 regulatory machinery of the host (44). As a particularly relevant example, systems
163 developed in the past for transgene expression caused severe growth and developmental
164 defects in *Arabidopsis* and *Nicotiana benthamiana* (45, 46). Therefore, it is paramount to

165 develop regulatory tools to control transgene expression that minimizes the impact on
166 endogenous plant machinery/physiology, while maintaining the modularity and scalability
167 of synthetic approaches in general.

168

169 A potential solution to this problem is to develop orthogonal 'parts' that of necessity
170 function independently of endogenous regulation by the host. To this end, we set out to
171 develop a fully integrated Orthogonal Control System (OCS) based on orthogonal
172 synthetic promoters driven by an Artificial Transcription Factor (ATF). We started with
173 the deactivated form of the Cas9 protein (dCas9) fused to the transcriptional activator
174 domain VP64 as a highly programmable ATF (26, 27). While dCas9:VP64 has previously
175 been shown to upregulate the expression of endogenous genes via specific guide RNAs
176 (gRNAs) that target the promoter region upstream of those genes (25, 47), this strategy
177 has not been utilized for the construction of a fully orthogonal system in which custom
178 promoters can be similarly regulated. Here we develop a suite of synthetic promoters
179 (pATFs, promoter for Artificial Transcription Factor) in which each promoter has a similar
180 modular architecture: varying number of repeats of gRNA binding sites followed by a
181 minimal 35S promoter (33, 34). This system is inherently scalable, since new binding
182 sites bound by new gRNAs can be built at will. The complete list of parts (promoters,
183 genes and terminators) is provided in **Supplementary Table 1**.

184

185 We initially varied the number of gRNA binding sites (3 and 4) upstream of the minimal
186 35S promoter, and analyzed expression of the reporter using transient assay in *Nicotiana*

187 *benthamiana*. Three repeats provided the best expression of the reporter gene without
188 significant background (**Fig 3A**). The promoter architecture was further assayed for leaky
189 expression by generating pATF:YFP/BFP/RFP constructs and expressing gRNA
190 constitutively in the absence of dCas9:VP64 (**Fig 3A**). None of these constructs show
191 expression above background (**Fig 3B and 3C**). However, upon the addition of
192 constitutively expressed dCas9:VP64 cassette to the circuit, induction of reporter protein
193 expression was observed (**Fig. 3B and 3C**). Each pATF demonstrated comparable levels
194 of expression (pATF1:YFP - 3-fold, pATF3:BFP - 6-fold and pATF4:RFP - 2 fold)
195 compared to that obtained from the regular 35S promoter (6-fold; **Fig 2B**). The basic
196 features of the pATF and corresponding gRNAs can thus form the basis for the OCS and
197 should allow us to predictably control reporter and other gene circuits. The complete list
198 of assembled OCS circuits is provided in **Supplementary Table 2**; as the reader will see,
199 OCS circuitry can be organized in terms of increasing complexity and demonstrates how
200 the Design-Built-Test approach can be used to empirically generate ever more
201 substantive plant phenotypes.

202 In order to show that the OCS designs could also function in stable transgenic *Arabidopsis*
203 *thaliana* lines, we assembled the OCS 1-1 and 4-1 circuits (**Supplementary Table 2**;
204 constitutive YFP and luciferase expression, respectively) in an *Agrobacterium* expression
205 vector containing with a kanamycin selectable marker as described previously. These
206 OCS constructs were successfully transformed into *Arabidopsis thaliana* plants (**Fig 4A**).
207 As expected, the OCS 1-1 T₁ plants exhibited constitutive YFP expression (**Fig 4B**) while
208 the OCS 4-1 plants were imaged (as described in **Methods**) and the constitutive

209 expression of luciferase was confirmed (**Fig 4C, 4D**). Thus, the modular circuits
210 assembled function in two species, as infiltrates in *Nicotiana* and as transgenics in
211 *Arabidopsis*.

212

213 **Inducible gene expression system via the OCS framework**

214

215 The ability to precisely regulate the activity of the transgenes/circuit components based
216 on specific input stimuli is a key feature in programmable synthetic circuits (48, 49). In
217 order to enable orthogonal control of induction, we designed gRNA expression cassettes
218 to produce functional gRNAs from inducible Pol II promoters. To prevent nuclear export
219 of gRNAs due to capping and polyadenylation, we used the hammerhead ribozyme
220 (HHR) and Hepatitis Delta Virus (HDV) to cleave the 5' and the 3' ends of the gRNA,
221 respectively. This strategy has been previously shown to lead to the expression of
222 functional gRNAs from Pol II promoters, with activity similar to those driven by the Pol III
223 (U6) promoter (50, 51).

224

225 To proof the ribozyme processed gRNA constructs, OCS circuits were assembled where
226 gRNAs were either expressed from a U6 promoter (OCS 1-1) or the 35S promoter (OCS
227 1-5), and could subsequently activate the transcription and expression of reporter genes
228 (YFP) (**Fig 5A**). For both OCS circuits, downstream reporter gene expression was
229 observed, at similar levels (**Fig. 5B**). The specific levels of gRNA obtained in each case
230 were analyzed using qRT-PCR (**Fig 5C and 5D**), and as expected the level of gRNA from

231 the strong Pol II (35S) driven expression was higher than those obtained with the U6
232 promoter while similar levels of reporter expression were observed for both cases, thus
233 demonstrating that this Pol II driven gRNA expression strategy can be effectively used for
234 OCS activation (**Fig 5E**). For both these constructs the expression of hdCas9 (human
235 codon optimized dCas9) was also confirmed via Western blot analysis (**Fig S2**).

236 In order to demonstrate that the Pol II-driven gRNAs could be used as part of an inducible
237 OCS we used the well-characterized synthetic EBS promoter containing the EIN3 binding
238 (52), and placed YFP under the downstream control of the ATF (via pATF-1) (**Fig 6A**).
239 This circuit (OCS1-9) should be inducible by the volatile organic compound (VOC)
240 ethylene, which is produced from its precursor ACC (1-aminocyclopropane-1-carboxylic
241 acid). Time-dependent expression of YFP is observed in response to 10uM ACC
242 induction (**Fig 6B**). Both the gRNA-1 and YFP expression levels were quantified before
243 and after induction by qRT-PCR, a maximum of 3-fold induction was observed for both
244 cases (**Fig 6C and 6D**). Thus, this demonstrates that the activity from synthetic promoters
245 can be controlled via the selective expression of the corresponding gRNAs.

246

247 **Construction of a panel of mutually orthogonal synthetic promoters**

248

249 Lack of multiplexed control of transgenes has been a major factor limiting the
250 development of synthetic circuits in plants (5, 6). Multiplexed regulation in turn requires
251 a panel of mutually orthogonal promoters and control elements that can operate
252 simultaneously (5, 6). Our strategy for synthetic promoter design naturally leads to the

253 generation of expression cassettes that are not only orthogonal to the host but are also
254 mutually orthogonal. The degree of orthogonality can be tuned at will via the sequence
255 design of the multiple gRNA components. By simply minimizing homology between
256 gRNAs, we constructed two additional promoters similar to the architecture of pATF-1, in
257 which gRNA binding sites were followed by a minimal 35S promoter (pATF-3 and pATF-
258 4). The orthogonality of these promoters was assayed by assembling expression
259 constructs in which each synthetic promoter controlled the production of a unique
260 fluorescent reporter (pATF-1: YFP, pATF-3: RFP and pATF-4: BFP). The respective
261 gRNAs (gRNA-1, gRNA-3 and gRNA-4) were separately transcribed from a U6 promoter
262 (**Fig 7A**). When expression constructs were infiltrated into *Nicotiana benthamiana*, each
263 of the synthetic promoters was specifically upregulated only when its corresponding
264 gRNA was expressed; no background was detected from the remaining two synthetic
265 promoters. (**Fig 7B and 7C**).

266

267 **Construction of complex ratiometric circuits**

268

269 Now that we have a suite of mutually orthogonal promoters, we sought to construct simple
270 circuits where the activity of each promoter could be independently controlled. Three
271 separate reporter proteins were used to simultaneously monitor the activity of two
272 promoters: pATF-1 with YFP, while both RFP and BFP were under the control of the
273 pATF-3. By leveraging the designed, orthogonal behavior of these promoters it proved
274 possible to construct a ratiometric circuit wherein the activity of pATF-1, and hence YFP

275 expression, was under the control of ethylene (via ACC), while pATF-3 constitutively
276 drove the expression of RFP and BFP (**Fig 8A**). As expected, the addition of 10uM ACC,
277 induced the expression of YFP from the pATF-1 promoter (3-fold), while the expression
278 of the other reporters remained constant (**Fig 8B and 8C**). The ratiometric response was
279 further validated by qRT-PCR; pATF-1 was induced 3-fold following a similar increase in
280 expression of gRNA-1 while there were no changes observed in the transcription of the
281 other two reporter genes (**Fig 8B and 8C**). The predictable behavior of the designed,
282 artificial control elements in the ratiometric circuit is one of the first examples of complex
283 circuitry to be described in plants, and demonstrates uniquely how natural metabolism
284 and regulatory circuitry can be interfaced with free-standing orthogonal control systems.

285

286

287 **Discussion**

288

289 Transcriptional orthogonality is one of the bedrocks for circuit construction in synthetic
290 biology, and generally serves as the basis for the bottom-up construction of complex
291 circuitry for predictable dynamics (7, 10, 17). For eukaryotes the construction of multiple
292 promoter elements is hindered by the typically complex regulatory sequences that lie
293 upstream and within promoters (53-55).

294

295 The design of synthetic eukaryotic promoters has traditionally implemented a common
296 architecture, where a strong transcriptional initiation region is cloned downstream of

297 orthogonal DNA binding operator sequences and the latter serve as landing pads for
298 synthetic transcription factors (23). The engineered transcription factors have typically
299 consisted of DNA binding proteins (i.e., prokaryotic DNA binding proteins like TetR, LacI,
300 LexA and PhIF (56-58)) fused to well characterized transcriptional activation domain like
301 VP64. With the advent of programmable DNA binding proteins like zinc finger proteins
302 and TALEs the repertoire of synthetic promoters greatly increased (23, 24, 59, 60). That
303 said, each new synthetic promoter still requires the construction and characterization of
304 its own unique transcription factor (23, 60, 61).

305

306 These bottlenecks can be circumvented by the use of the highly programmable RNA-
307 guided DNA binding protein dCas9 (26). The dCas9 RNP fused to transcription activation
308 domains such as VP64 has been used for the upregulation of endogenous genes in a
309 wide variety of eukaryotic species like yeast, mammalian cells and plants (16, 25, 26,
310 62). Here, we have used adapted this 'universal' transcription factor to control the
311 expression of synthetic and orthogonal promoters without the need of addition of any
312 other factors. Using our modular framework, we were able to quickly design and
313 characterize a panel of mutually orthogonal promoters that could drive the production of
314 a variety of outputs, singly and in parallel, including different fluorescent proteins (GFP,
315 BFP, RFP and YFP) and luciferase.

316

317 The activities of dCas9 based transcription factors can potentially be controlled by simply
318 regulating the expression of their corresponding gRNAs (16, 17), enabling the coupling

319 of natural and synthetic transcription units, and thus natural and overlaid metabolic
320 responses. Here we have effectively used this strategy to couple ethylene sensing (via
321 known EIN3 binding sites) to synthetic (pATF) promoters. Moreover, by changing the
322 number and arrangement of gRNA binding sites synthetic promoters with different levels
323 of activation can be generated, providing further opportunities for design (63). While it
324 has been previously shown that a panel of minimal plant promoters can be used with
325 natural DNA binding sequences for modulating promoter strengths (20), the addition of
326 completely artificial, synthetic promoters as control elements should create opportunities
327 for increasing the specificity and strengths of engineered promoters.
328 Since our strategy for designing synthetic promoters is generalizable it is likely that even
329 more complex circuits can be built by simply incorporating other transcription factor
330 binding sites, or by changing the regulatory 'headpiece' on the dCas9 element (for
331 example, to a repressor), (64-66).

332

333 The stabilities of genetic circuitry in plants can be greatly modified by silencing and
334 recombination, amongst other mechanisms (40, 41, 43). In this regard, the artificial
335 promoter elements that we generate can potentially be crafted to avoid repetition (20),
336 and thus to better avoid silencing and recombination. As viable artificial promoter
337 sequences continue to accumulate, they can be compared and contrasted to identify
338 those that are least vulnerable to modification over time. The facile addition of new parts
339 to the standardize toolkit architecture, particularly terminators, will further increase

340 opportunities to avoid repetition in ways that again go well beyond what is possible by
341 relying on just a few well-characterized endogenous elements alone.

342

343 The implementation of orthogonal control systems in plants can be used to limit cross-
344 talk between natural and overlaid regulatory elements, allowing more precise response
345 to a variety of inputs, from VOCs to hormones to temperature, water, and nutrients. The
346 use of orthogonal control systems to enable more precise responses to pathogenesis is
347 especially intriguing given the presence of R genes that are specifically responsive to
348 individual pathogens (effector triggered immunity, ETI) (67). The architecture we have
349 developed is fully generalizable, and can potentially be expanded to non-model plants
350 and other eukaryotic species such as yeast and mammalian cells by the use of
351 appropriate transcription initiation regions under the control of similar gRNA sequences
352 binding sites (68).

353

354 **Conclusion**

355 The design of synthetic promoters based on gRNAs and CRISPR-based transcription
356 factor (dCas9:VP64) is highly generalizable to large tracts of sequence space, allowing
357 Orthogonal Control Systems of increasing complexity to potentially be generated at will.
358 The ability to tie in several different basal features of plant molecular biology (Pol II and
359 Pol III promoters, ethylene regulation) to the OCS demonstrates multiple opportunities for
360 engineering at the system level. Moreover, given the fungibility of the core 35S CaMV

361 promoter elements, the derived synthetic promoters can potentially be utilized across a
362 variety of plant species.

363

364 **Materials and Methods**

365

366 ***Plasmid design and construction***

367

368 The plant expression vector was generated using the plasmid pICH86966
369 (Addgene#48075) as the backbone. The lacZ expression cassette was replaced with the
370 GFP dropout sequence (**Supplementary Table 2**) to make the plasmid compatible with
371 YTK architecture design. All parts described in **Supplementary Table 1**, were cloned
372 into the backbone pYTK001 (Addgene #65108). For the individual transcriptional units,
373 the backbone used was pYTK095 (Addgene #65202) along with the appropriate
374 connector sequences described in **Supplementary Table 3**. For the design of orthogonal
375 gRNAs, random 20-mers were generated that had a GC content of ~50%, and that were
376 at least 5 nucleotides away from all sequences in the *Nicotiana* and *Arabidopsis*
377 genomes. All oligonucleotides and gblocks were obtained from Integrated DNA
378 Technologies (IDT) unless otherwise stated.

379 For the construction of each genetic element namely promoters, coding sequences and
380 terminators, first they were checked for restriction sites for the following enzymes –
381 BsmBI, BsaI, NotI and DraIII. The restriction sites in the coding sequences were removed
382 by the use of synonymous codons while the other elements did not contain any of these

383 restriction sites. The complete list of parts and constructs are provided in **Supplementary**
384 **Table 1**. The part plasmids were cloned into a common vector where each genetic
385 element is flanked by Bsa1 restriction sites followed by appropriate overhangs
386 (**Supplementary Table 1**). For the assembly of both single TU or multi-TU, the following
387 procedure was used: 10 fmol of backbone plasmid and 20 fmol of parts/TUs were used
388 in a 10uL reaction with 1ul of 10x T4 ligase buffer along with 100 units of BsaI-v2 (single
389 TU) or Esp3I (multi-TU or parts) and 100 units of T7 DNA ligase. The cycling protocol
390 used is: 24 cycles of 3 min at 37°C (for digestion) and 5 min at 16°C (for ligation) followed
391 by a final digestion step at 37°C for 30min and the enzymes were heat inactivated 80°C
392 for 20 min. All constructs were transformed into DH10B cells, grown at 37°C using
393 standard chemical transformation procedures. The colonies that lack fluorescence were
394 inoculated and plasmids were extracted using Qiagen Miniprep kit according to the
395 manufacturer's instructions Plasmids were maintained as the following antibiotics
396 kanamycin (50ug/mL), chloramphenicol (34ug/mL) and carbenicillin (100ug/mL)
397 wherever required. The plasmids were sequence verified by Sanger sequencing (UT
398 Austin Genomic Sequencing and Analysis Facility). The correct constructs were then
399 transformed into *Agrobacterium tumefaciens* strain GV3101 (resistant to Gentamycin and
400 Rifampicin) and used either for transient expression in *Nicotiana benthamiana* or to
401 generate stable lines in *Arabidopsis thaliana*. The following enzymes were used for the
402 assemblies – BsaI-v2 (NEB #R3733S), Esp3I (NEB #R0734S) and T7 DNA ligase (NEB
403 #M0318S).
404

405 ***Plant material, bacterial infiltration***

406 *Nicotiana benthamiana* and *Arabidopsis thaliana* plants were grown in soil at 22°C, and
407 16 hr light period. For transient expression, three weeks old plants were syringe-infiltrated
408 with *Agrobacterium tumefaciens* strain GV3101 (OD₆₀₀ = 0.5) and leaves were imaged
409 under Olympus BX53 Digital Fluorescence Microscope or harvested for RNA and/or
410 protein analysis. To create stable transformation in *Arabidopsis*, floral dip method (69)
411 was used. T₁ plants were selected on half MS Kanamycin (50µg/ml) plates and the
412 selected T₁ plants were analyzed using an Olympus BX53 Digital Fluorescence
413 Microscope and a NightOwl imager for YFP expression and luciferase expression,
414 respectively. For circuits that constitutively expressed YFP (OCS1-1) and luciferase
415 (OCS4-1) no other obvious phenotypic differences were observed across numerous
416 individual plants.

417

418 ***RNA extraction and qRT-PCR***

419 RNA was extracted using TRIzol reagent (Ambion). 1µg total RNA was used to synthesize
420 cDNA. After DNaseI treatment to remove any DNA contamination, random primer mix
421 (NEB #S1330S) and M-MLV Reverse transcriptase (Invitrogen #28025-013) were used
422 for first strand synthesis. qRT-PCR was used to quantify the RNA prepared from transient
423 expression experiments. AzuraQuant qPCR Master Mix (Azura Genomics) was used with
424 initial incubation at 95 °C for 2 min followed by 40 cycles of 95 °C for 10 sec and 60 °C
425 for 30sec. Level of target RNA was calculated from the difference of threshold cycle (Ct)

426 values between reference (*5S rRNA*) and target gene using at least three independent
427 replicates

428

429 ***ACC treatment***

430 To check the induction of reporter in response to ACC in the plasmids containing
431 pEBS::YFP/RFP/BFP, *Nicotiana benthamiana* leaves were infiltrated with *Agrobacterium*;
432 after three days post infiltration, leaf discs were cut using cork borer and incubated in
433 either 0 μ M or 10 μ M ACC for four hours. Fluorescence microscopy was used to check
434 YFP expression after induction.

435

436 **Fluorescence and Luminescence imaging**

437 Fluorescence microscope images after *Agrobacterium* mediated transient expression of
438 YFP, BFP, RFP and GFP in *Nicotiana benthamiana* leaves were taken using an Olympus
439 BX53 Digital Fluorescence Microscope. For this purpose, leaf discs were cut using cork
440 borer from the area which was infiltrated. Images were taken using either 10X objective
441 lens using the default filters for YFP (500/535nm), BFP (385/448nm), and RFP
442 (560/630nm). The UV filter (350/460nm) was used to take GFP images. The exposure
443 and gain setting were kept constant for each filter within each experiment to compare
444 multiple leaf discs (3 to 6). In all the experiments a leaf disc from a leaf which was not
445 infiltrated with *Agrobacterium* was used as a negative control in order to account for
446 background fluorescence. All experiments were performed at least three times
447 independently as indicated in the Results.

448 Expression of luciferase was detected using NightOwl II LB 983 *in vivo* imaging system
449 ([https://www.berthold.com/en/bioanalytic/products/in-vivo-imaging-systems/nightowl-](https://www.berthold.com/en/bioanalytic/products/in-vivo-imaging-systems/nightowl-lb983/)
450 [lb983/](https://www.berthold.com/en/bioanalytic/products/in-vivo-imaging-systems/nightowl-lb983/)). Leaves/plants were sprayed with 100 μ M D-luciferin, Potassium salt (GoldBio
451 #LUCK-300). After 5 min of incubation, images were taken in the NightOwl II LB 983.
452 Images were captured with a backlit NightOWL LB 983 NC 100 CCD camera. Photons
453 emitted from luciferase were collected and integrated for a 2 min period. A pseudocolor
454 luminescent image from blue (least intense) to red (most intense), representing the
455 distribution of the detected photons emitted from active luciferase was generated using
456 Indigo software (Berthold Technologies).

457

458 ***Western blot***

459 Total protein was extracted using urea-based denaturing buffer (100 mM NaH₂PO₄, 8 M
460 urea, and 10 mM Tris-HCl, pH 8.0) and used for immunoblot analysis to check the
461 expression. The proteins were fractionated by 8% SDS-PAGE gel and transferred to a
462 polyvinylidene difluoride (PVDF) membrane using a transfer apparatus according to the
463 manufacturer's protocols (Bio-Rad). The membrane was treated with 5% nonfat milk in
464 PBS-T for 10 min for blocking, and then incubated with Cas9 antibody (Santa cruz, 7A9-
465 3A3, 1:500) at 4 °C for overnight. After incubation, the membrane was washed three times
466 for 5 min and incubated with horseradish peroxidase-conjugated anti-mouse (1:10000)
467 for 2 h. The Blot was washed with PBS-T three times and detected with the ECL system
468 (Thermo scientific, lot# SE251206).

469

470 **Declarations**

471

472 **Ethics approval and consent to participate**

473 Not Applicable

474

475 **Consent for publication**

476 Not Applicable

477

478 **Availability of data and materials**

479 The datasets during and/or analysed during the current study available from the
480 corresponding author on reasonable request

481

482 **Competing interests**

483 The authors declare no competing interests.

484

485 **Funding**

486 This work was supported by the Defense Advanced Research Projects Agency (DARPA)
487 agreement HR00111820048 to AE and SS. The content of the information does not
488 necessarily reflect the position or the policy of the Government, and no official
489 endorsement should be inferred. This work was also supported by Welch Foundation
490 grant (F-1654) to ADE.

491

492 **Authors' contributions**

493 SK, SS and AE conceived of the project. SK designed the framework and the basic
494 elements of OCS with input from EG, JG and SS. SK and YB assembled all constructs.
495 YB, NR and JK performed all the testing in *Nicotiana* with input from SS. All authors
496 contributed with the preparation of figures. SK, YB, JK, SS and AE wrote the manuscript
497 with input from all authors.

498

499 **Acknowledgments**

500 We would also like to thank the Qiao lab (UT Austin) for providing details regarding the
501 ethylene induction of the OCS constructs.

502

503 **Supplementary Information** includes

504

505 **Fig S1:** Workflow describing the assembly of single and multiple transcriptional units
506 (TUs) in a plant expression vector; **Fig S2:** Western blot to analyze the expression of
507 dCas9:VP64 in OCS constructs – OCS1-1 and OCS 1-5

508 **Table S1:** List of all genetic parts used for the construction of OCS constructs

509 **Table S2:** List of all OCS constructs

510 **Table S3:** List of all Addgene plasmids used in this work

511

512

513 **References**

514

- 515 1. Tolle F, Stucheli P, Fussenegger M. Genetic circuitry for personalized human cell therapy.
516 *Current opinion in biotechnology*. 2019;59:31-8.
- 517 2. Scheller L, Fussenegger M. From synthetic biology to human therapy: engineered
518 mammalian cells. *Current opinion in biotechnology*. 2019;58:108-16.
- 519 3. Sedlmayer F, Aibel D, Fussenegger M. Synthetic gene circuits for the detection,
520 elimination and prevention of disease. *Nature biomedical engineering*. 2018;2(6):399-415.
- 521 4. Riglar DT, Silver PA. Engineering bacteria for diagnostic and therapeutic applications.
522 *Nature reviews Microbiology*. 2018;16(4):214-25.
- 523 5. Kassaw TK, Donayre-Torres AJ, Antunes MS, Morey KJ, Medford JI. Engineering synthetic
524 regulatory circuits in plants. *Plant science : an international journal of experimental plant biology*.
525 2018;273:13-22.

- 526 6. de Lange O, Klavins E, Nemhauser J. Synthetic genetic circuits in crop plants. *Current*
527 *opinion in biotechnology*. 2018;49:16-22.
- 528 7. Nielsen AA, Der BS, Shin J, Vaidyanathan P, Paralanov V, Strychalski EA, et al. Genetic
529 circuit design automation. *Science (New York, NY)*. 2016;352(6281):aac7341.
- 530 8. Medford JI, Prasad A. Towards programmable plant genetic circuits. *The Plant journal :*
531 *for cell and molecular biology*. 2016;87(1):139-48.
- 532 9. Fonseca JP, Bonny AR, Kumar GR, Ng AH, Town J, Wu QC, et al. A Toolkit for Rapid Modular
533 Construction of Biological Circuits in Mammalian Cells. *ACS synthetic biology*. 2019;8(11):2593-
534 606.
- 535 10. Brophy JA, Voigt CA. Principles of genetic circuit design. *Nature methods*. 2014;11(5):508-
536 20.
- 537 11. Mutalik VK, Guimaraes JC, Cambrey G, Lam C, Christoffersen MJ, Mai QA, et al. Precise
538 and reliable gene expression via standard transcription and translation initiation elements.
539 *Nature methods*. 2013;10(4):354-60.
- 540 12. Weinberg BH, Pham NTH, Caraballo LD, Lozano T, Engel A, Bhatia S, et al. Large-scale
541 design of robust genetic circuits with multiple inputs and outputs for mammalian cells. *Nature*
542 *biotechnology*. 2017;35(5):453-62.
- 543 13. Basu S, Gerchman Y, Collins CH, Arnold FH, Weiss R. A synthetic multicellular system for
544 programmed pattern formation. *Nature*. 2005;434(7037):1130-4.
- 545 14. Gardner TS, Cantor CR, Collins JJ. Construction of a genetic toggle switch in *Escherichia*
546 *coli*. *Nature*. 2000;403(6767):339-42.
- 547 15. Elowitz MB, Leibler S. A synthetic oscillatory network of transcriptional regulators.
548 *Nature*. 2000;403(6767):335-8.
- 549 16. Kim H, Bojar D, Fussenegger M. A CRISPR/Cas9-based central processing unit to program
550 complex logic computation in human cells. *Proceedings of the National Academy of Sciences of*
551 *the United States of America*. 2019;116(15):7214-9.
- 552 17. Gander MW, Vrana JD, Voje WE, Carothers JM, Klavins E. Digital logic circuits in yeast with
553 CRISPR-dCas9 NOR gates. *Nature communications*. 2017;8:15459.
- 554 18. Weber W, Fussenegger M. Engineering of synthetic mammalian gene networks.
555 *Chemistry & biology*. 2009;16(3):287-97.
- 556 19. Kramer BP, Fussenegger M. Hysteresis in a synthetic mammalian gene network.
557 *Proceedings of the National Academy of Sciences of the United States of America*.
558 2005;102(27):9517-22.
- 559 20. Belcher MS, Vuu KM, Zhou A, Mansoori N, Agosto Ramos A, Thompson MG, et al. Design
560 of orthogonal regulatory systems for modulating gene expression in plants. *Nature chemical*
561 *biology*. 2020;16(8):857-65.
- 562 21. Schaumberg KA, Antunes MS, Kassaw TK, Xu W, Zalewski CS, Medford JI, et al.
563 Quantitative characterization of genetic parts and circuits for plant synthetic biology. *Nature*
564 *methods*. 2016;13(1):94-100.
- 565 22. Brückner K, Schäfer P, Weber E, Grützner R, Marillonnet S, Tissier A. A library of synthetic
566 transcription activator-like effector-activated promoters for coordinated orthogonal
567 gene expression in plants. *The Plant journal : for cell and molecular biology*. 2015;82(4):707-16.
- 568 23. Khalil AS, Lu TK, Bashor CJ, Ramirez CL, Pyenson NC, Joung JK, et al. A synthetic biology
569 framework for programming eukaryotic transcription functions. *Cell*. 2012;150(3):647-58.

- 570 24. Bae KH, Kwon YD, Shin HC, Hwang MS, Ryu EH, Park KS, et al. Human zinc fingers as
571 building blocks in the construction of artificial transcription factors. *Nature biotechnology*.
572 2003;21(3):275-80.
- 573 25. Li Z, Zhang D, Xiong X, Yan B, Xie W, Sheen J, et al. A potent Cas9-derived gene activator
574 for plant and mammalian cells. *Nature plants*. 2017;3(12):930-6.
- 575 26. Perez-Pinera P, Kocak DD, Vockley CM, Adler AF, Kabadi AM, Polstein LR, et al. RNA-guided
576 gene activation by CRISPR-Cas9-based transcription factors. *Nature methods*. 2013;10(10):973-
577 6.
- 578 27. Chavez A, Tuttle M, Pruitt BW, Ewen-Campen B, Chari R, Ter-Ovanesyan D, et al.
579 Comparison of Cas9 activators in multiple species. *Nature methods*. 2016;13(7):563-7.
- 580 28. Lee ME, DeLoache WC, Cervantes B, Dueber JE. A Highly Characterized Yeast Toolkit for
581 Modular, Multipart Assembly. *ACS synthetic biology*. 2015;4(9):975-86.
- 582 29. Engler C, Youles M, Gruetzner R, Ehnert TM, Werner S, Jones JD, et al. A golden gate
583 modular cloning toolbox for plants. *ACS synthetic biology*. 2014;3(11):839-43.
- 584 30. Weber E, Engler C, Gruetzner R, Werner S, Marillonnet S. A modular cloning system for
585 standardized assembly of multigene constructs. *PLoS one*. 2011;6(2):e16765.
- 586 31. Banta LM, Montenegro M. *Agrobacterium and Plant Biotechnology*. In: Tzfira T, Citovsky
587 V, editors. *Agrobacterium: From Biology to Biotechnology*. New York, NY: Springer New York;
588 2008. p. 73-147.
- 589 32. Berg RH, Beachy RN. Fluorescent protein applications in plants. *Methods Cell Biol*.
590 2008;85:153-77.
- 591 33. Benfey PN, Chua NH. The Cauliflower Mosaic Virus 35S Promoter: Combinatorial
592 Regulation of Transcription in Plants. *Science (New York, NY)*. 1990;250(4983):959-66.
- 593 34. Odell JT, Nagy F, Chua NH. Identification of DNA sequences required for activity of the
594 cauliflower mosaic virus 35S promoter. *Nature*. 1985;313(6005):810-2.
- 595 35. Kerppola TK. Bimolecular Fluorescence Complementation (BiFC) Analysis as a Probe of
596 Protein Interactions in Living Cells. *Annual Review of Biophysics*. 2008;37(1):465-87.
- 597 36. Tindall AJ, Waller J, Greenwood M, Gould PD, Hartwell J, Hall A. A comparison of high-
598 throughput techniques for assaying circadian rhythms in plants. *Plant Methods*. 2015;11(1):32.
- 599 37. Xiong TC, Sanchez F, Briat J-F, Gaymard F, Dubos C. Spatio-Temporal Imaging of Promoter
600 Activity in Intact Plant Tissues. In: Hehl R, editor. *Plant Synthetic Promoters: Methods and*
601 *Protocols*. New York, NY: Springer New York; 2016. p. 103-10.
- 602 38. Xu G, Greene GH, Yoo H, Liu L, Marqués J, Motley J, et al. Global translational
603 reprogramming is a fundamental layer of immune regulation in plants. *Nature*.
604 2017;545(7655):487-90.
- 605 39. Zhou M, Wang W, Karapetyan S, Mwimba M, Marqués J, Buchler NE, et al. Redox rhythm
606 reinforces the circadian clock to gate immune response. *Nature*. 2015;523:472.
- 607 40. Vaillant I, Schubert I, Tourmente S, Mathieu O. MOM1 mediates DNA-methylation-
608 independent silencing of repetitive sequences in *Arabidopsis*. *EMBO Rep*. 2006;7(12):1273-8.
- 609 41. Matzke MA, Mette MF, Matzke AJ. Transgene silencing by the host genome defense:
610 implications for the evolution of epigenetic control mechanisms in plants and vertebrates. *Plant*
611 *Mol Biol*. 2000;43(2-3):401-15.

- 612 42. Ni M, Cui D, Einstein J, Narasimhulu S, Vergara CE, Gelvin SB. Strength and tissue
613 specificity of chimeric promoters derived from the octopine and mannopine synthase genes. *The*
614 *Plant Journal*. 1995;7(4):661-76.
- 615 43. Matzke MA, Primig M, Trnovsky J, Matzke AJ. Reversible methylation and inactivation of
616 marker genes in sequentially transformed tobacco plants. *Embo j*. 1989;8(3):643-9.
- 617 44. Cardinale S, Arkin AP. Contextualizing context for synthetic biology – identifying causes of
618 failure of synthetic biological systems. *Biotechnology Journal*. 2012;7(7):856-66.
- 619 45. Kang H-G, Fang Y, Singh KB. A glucocorticoid-inducible transcription system causes severe
620 growth defects in *Arabidopsis* and induces defense-related genes. *The Plant Journal*.
621 1999;20(1):127-33.
- 622 46. Amirsadeghi S, McDonald AE, Vanlerberghe GC. A glucocorticoid-inducible gene
623 expression system can cause growth defects in tobacco. *Planta*. 2007;226(2):453-63.
- 624 47. Lowder LG, Paul JW, 3rd, Qi Y. Multiplexed Transcriptional Activation or Repression in
625 Plants Using CRISPR-dCas9-Based Systems. *Methods in molecular biology* (Clifton, NJ).
626 2017;1629:167-84.
- 627 48. Bayer TS, Smolke CD. Programmable ligand-controlled riboregulators of eukaryotic gene
628 expression. *Nature Biotechnology*. 2005;23(3):337-43.
- 629 49. Kotula JW, Kerns SJ, Shaket LA, Siraj L, Collins JJ, Way JC, et al. Programmable bacteria
630 detect and record an environmental signal in the mammalian gut. *Proceedings of the National*
631 *Academy of Sciences*. 2014;111(13):4838.
- 632 50. Jacobs JZ, Ciccaglione KM, Tournier V, Zaratiegui M. Implementation of the CRISPR-Cas9
633 system in fission yeast. *Nature Communications*. 2014;5(1):5344.
- 634 51. Nissim L, Perli SD, Fridkin A, Perez-Pinera P, Lu TK. Multiplexed and programmable
635 regulation of gene networks with an integrated RNA and CRISPR/Cas toolkit in human cells.
636 *Molecular cell*. 2014;54(4):698-710.
- 637 52. Cruz AB, Bianchetti RE, Alves FRR, Purgatto E, Peres LEP, Rossi M, et al. Light, Ethylene
638 and Auxin Signaling Interaction Regulates Carotenoid Biosynthesis During Tomato Fruit Ripening.
639 *Frontiers in Plant Science*. 2018;9(1370).
- 640 53. Lelli KM, Slattery M, Mann RS. Disentangling the many layers of eukaryotic transcriptional
641 regulation. *Annual review of genetics*. 2012;46:43-68.
- 642 54. Ellwood K, Huang W, Johnson R, Carey M. Multiple layers of cooperativity regulate
643 enhanceosome-responsive RNA polymerase II transcription complex assembly. *Mol Cell Biol*.
644 1999;19(4):2613-23.
- 645 55. Chen L. Combinatorial gene regulation by eukaryotic transcription factors. *Curr Opin*
646 *Struct Biol*. 1999;9(1):48-55.
- 647 56. Urlinger S, Baron U, Thellmann M, Hasan MT, Bujard H, Hillen W. Exploring the sequence
648 space for tetracycline-dependent transcriptional activators: novel mutations yield expanded
649 range and sensitivity. *Proceedings of the National Academy of Sciences of the United States of*
650 *America*. 2000;97(14):7963-8.
- 651 57. Bellí G, Garí E, Piedrafita L, Aldea M, Herrero E. An activator/repressor dual system allows
652 tight tetracycline-regulated gene expression in budding yeast. *Nucleic Acids Research*.
653 1998;26(4):942-7.

654 58. Gossen M, Bujard H. Tight control of gene expression in mammalian cells by tetracycline-
655 responsive promoters. *Proceedings of the National Academy of Sciences of the United States of*
656 *America*. 1992;89(12):5547-51.

657 59. Perez-Pinera P, Ousterout DG, Brunger JM, Farin AM, Glass KA, Guilak F, et al. Synergistic
658 and tunable human gene activation by combinations of synthetic transcription factors. *Nature*
659 *methods*. 2013;10(3):239-42.

660 60. Li Y, Moore R, Guinn M, Bleris L. Transcription activator-like effector hybrids for
661 conditional control and rewiring of chromosomal transgene expression. *Sci Rep*. 2012;2:897.

662 61. Cermak T, Doyle EL, Christian M, Wang L, Zhang Y, Schmidt C, et al. Efficient design and
663 assembly of custom TALEN and other TAL effector-based constructs for DNA targeting. *Nucleic*
664 *Acids Research*. 2011;39(12):e82.

665 62. Lowder LG, Zhang D, Baltes NJ, Paul JW, 3rd, Tang X, Zheng X, et al. A CRISPR/Cas9 Toolbox
666 for Multiplexed Plant Genome Editing and Transcriptional Regulation. *Plant physiology*.
667 2015;169(2):971-85.

668 63. Kocak DD, Josephs EA, Bhandarkar V, Adkar SS, Kwon JB, Gersbach CA. Increasing the
669 specificity of CRISPR systems with engineered RNA secondary structures. *Nature biotechnology*.
670 2019;37(6):657-66.

671 64. Pandelakis M, Delgado E, Ebrahimkhani MR. CRISPR-Based Synthetic Transcription
672 Factors In Vivo: The Future of Therapeutic Cellular Programming. *Cell Syst*. 2020;10(1):1-14.

673 65. Yeo NC, Chavez A, Lance-Byrne A, Chan Y, Menn D, Milanova D, et al. An enhanced CRISPR
674 repressor for targeted mammalian gene regulation. *Nature methods*. 2018;15(8):611-6.

675 66. Kwon DY, Zhao YT, Lamonica JM, Zhou Z. Locus-specific histone deacetylation using a
676 synthetic CRISPR-Cas9-based HDAC. *Nature communications*. 2017;8:15315.

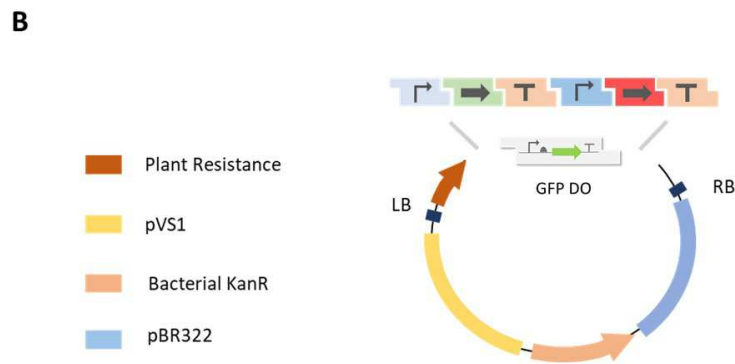
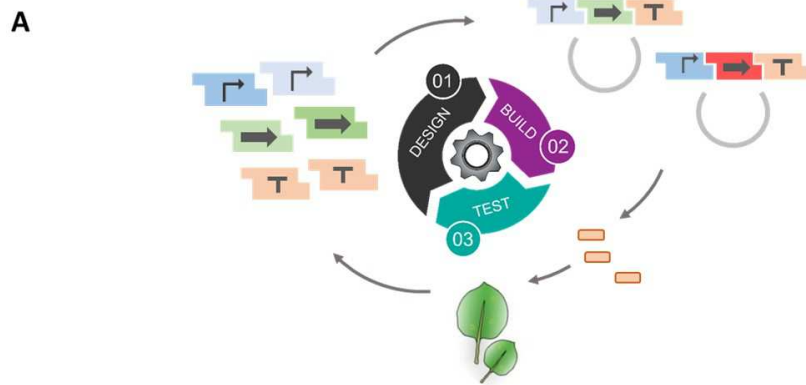
677 67. Gonzalez TL, Liang Y, Nguyen BN, Staskawicz BJ, Loqué D, Hammond MC. Tight regulation
678 of plant immune responses by combining promoter and suicide exon elements. *Nucleic Acids*
679 *Research*. 2015;43(14):7152-61.

680 68. Farzadfard F, Perli SD, Lu TK. Tunable and multifunctional eukaryotic transcription factors
681 based on CRISPR/Cas. *ACS synthetic biology*. 2013;2(10):604-13.

682 69. Zhang X, Henriques R, Lin S-S, Niu Q-W, Chua N-H. Agrobacterium-mediated
683 transformation of *Arabidopsis thaliana* using the floral dip method. *Nature Protocols*.
684 2006;1(2):641-6.

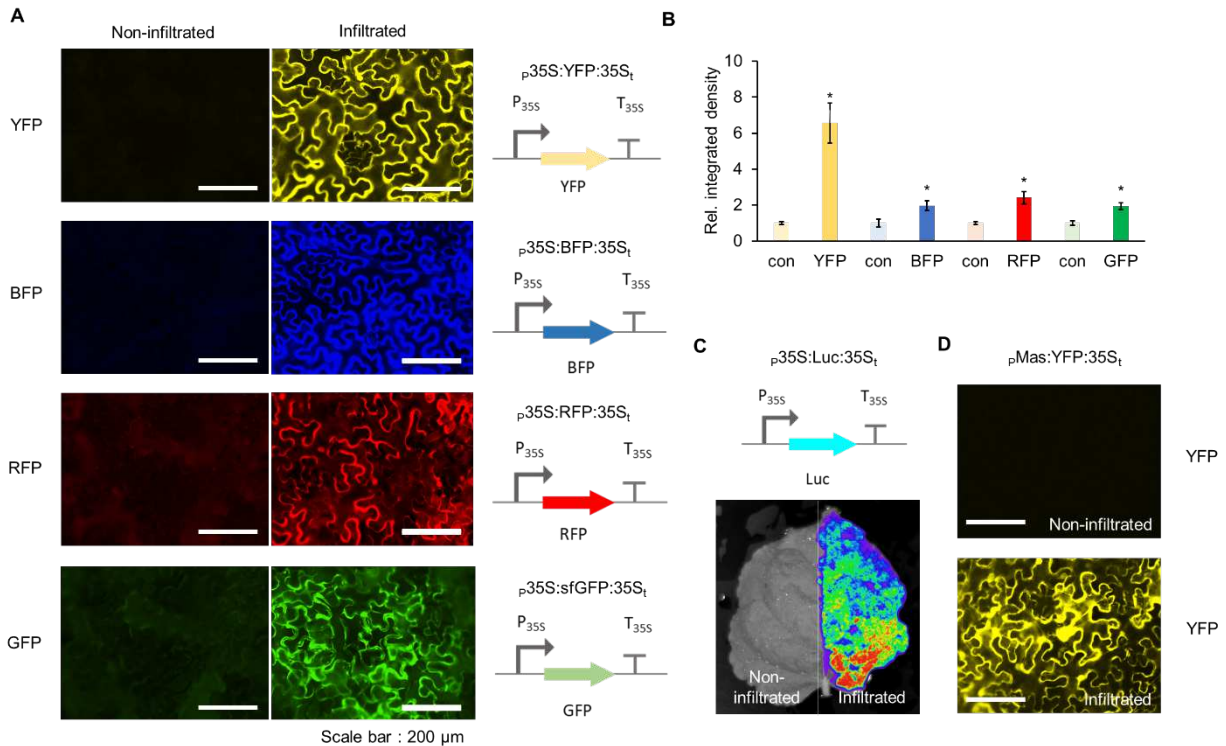
685

686



687
 688
 689
 690
 691
 692
 693
 694
 695
 696

Figure 1. Schematic overview of the design-build-test cycle **A.** Genetic elements such as promoters, genes and terminators are encoded as modular parts consisting of Bsal recognition sites flanked by specific overhangs to ensure the hierarchical assembly of transcriptional units. Once assembled, the constructs are transformed into Agrobacterium and the reporter expression is characterized in *Nicotiana benthamiana* leaf infiltrates **B.** Design of the shuttle vector backbone used for the assembly of constructs and subsequent propagation in *Agrobacterium*.



697

698

699 **Figure 2. Characterization of reporter constructs assembled using APT toolkit. A.**

700 Fluorescence microscope images showing *Agrobacterium* mediated transient expression

701 of YFP, BFP, RFP and GFP under the control of 35S promoter into *Nicotiana*

702 *benthamiana* leaves. Images on the left are from non-infiltrated leaves (negative control)

703 captured using the appropriate filter at same exposure and gain settings as was used for

704 the positive images on the right (**Material and Methods**). **B.** Relative integrated density

705 of each fluorescence signal (shown in panel A). Integrated density was measured using

706 image J software and normalized to that of a non-infiltrated control (con). Error bars: S.D.

707 (n=3, independent replicates). Asterisks indicate statistical significance in a student t-test

708 (P<0.05). **C.** Luminescence reporter luciferase expression shown by *Agrobacterium*

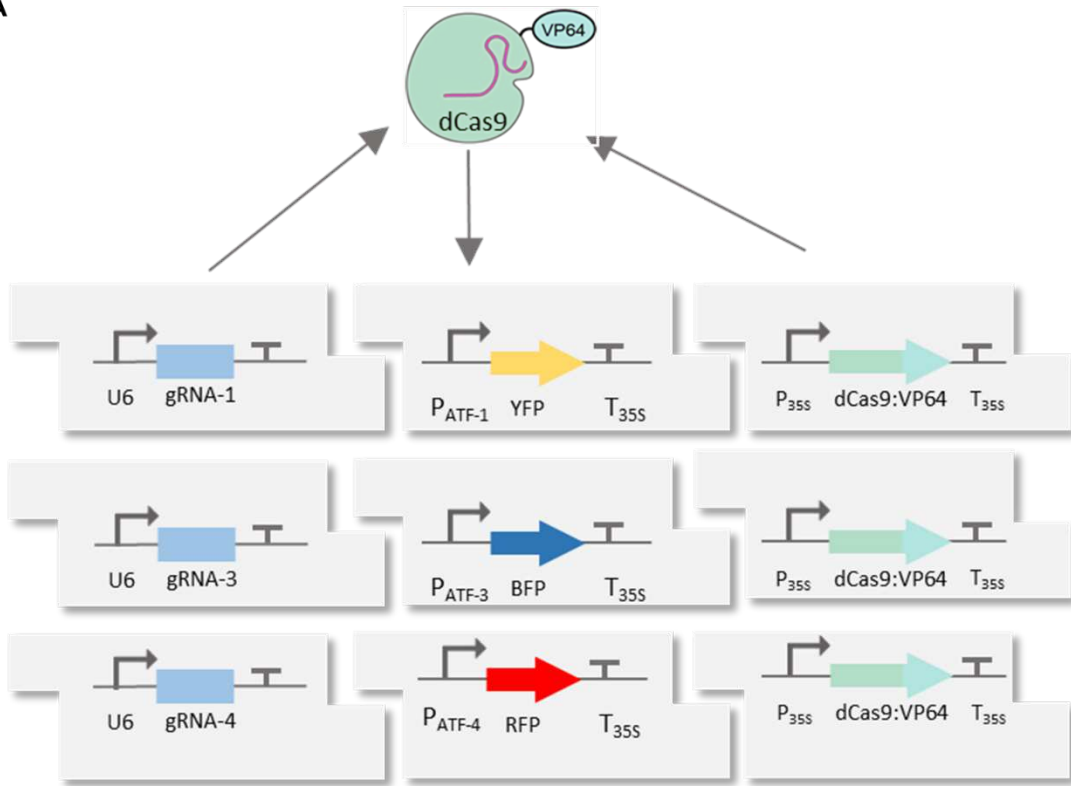
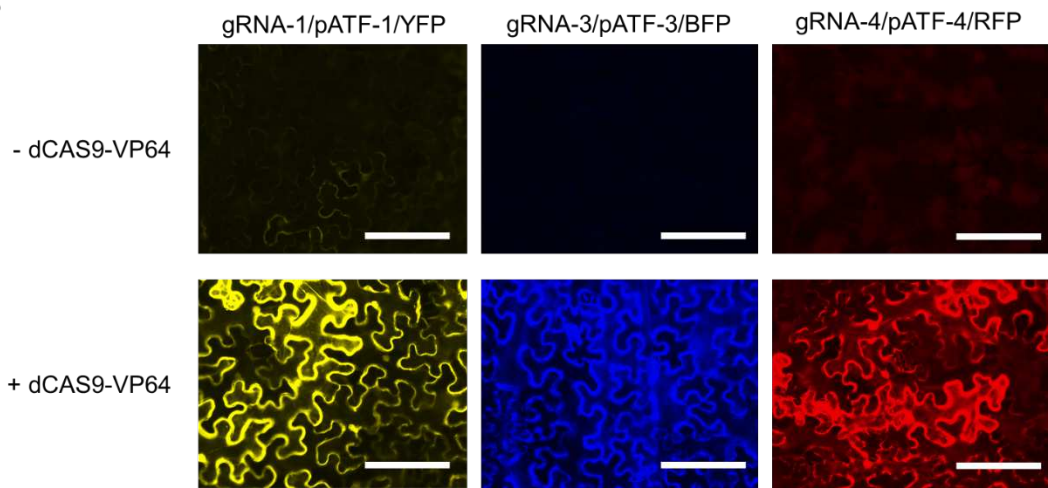
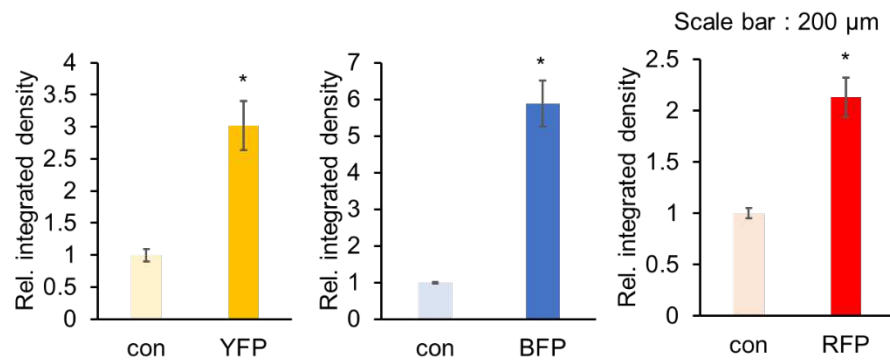
709 mediated transient expression of luciferase in *Nicotiana benthamiana* leaves. Left half of

710 the leaf was not infiltrated with *Agrobacterium*. **D.** Fluorescence microscope images

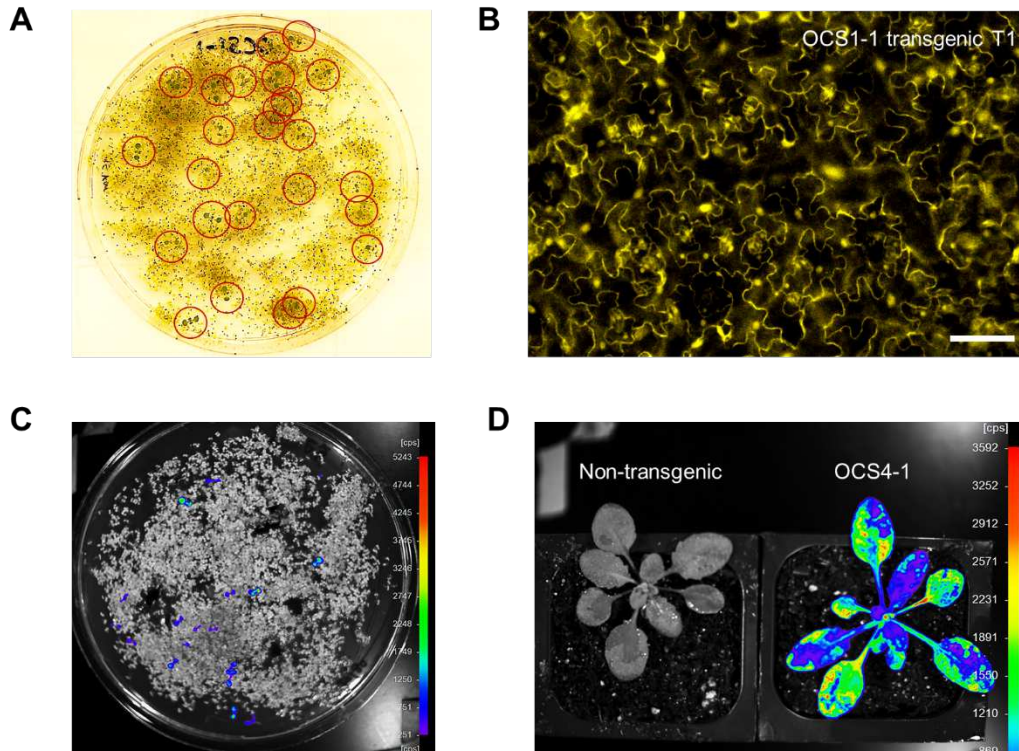
711 showing *Agrobacterium* mediated transient expression of YFP under MAS promoter in

712 *Nicotiana benthamiana* leaves. Image on the left is the brightfield image for the same

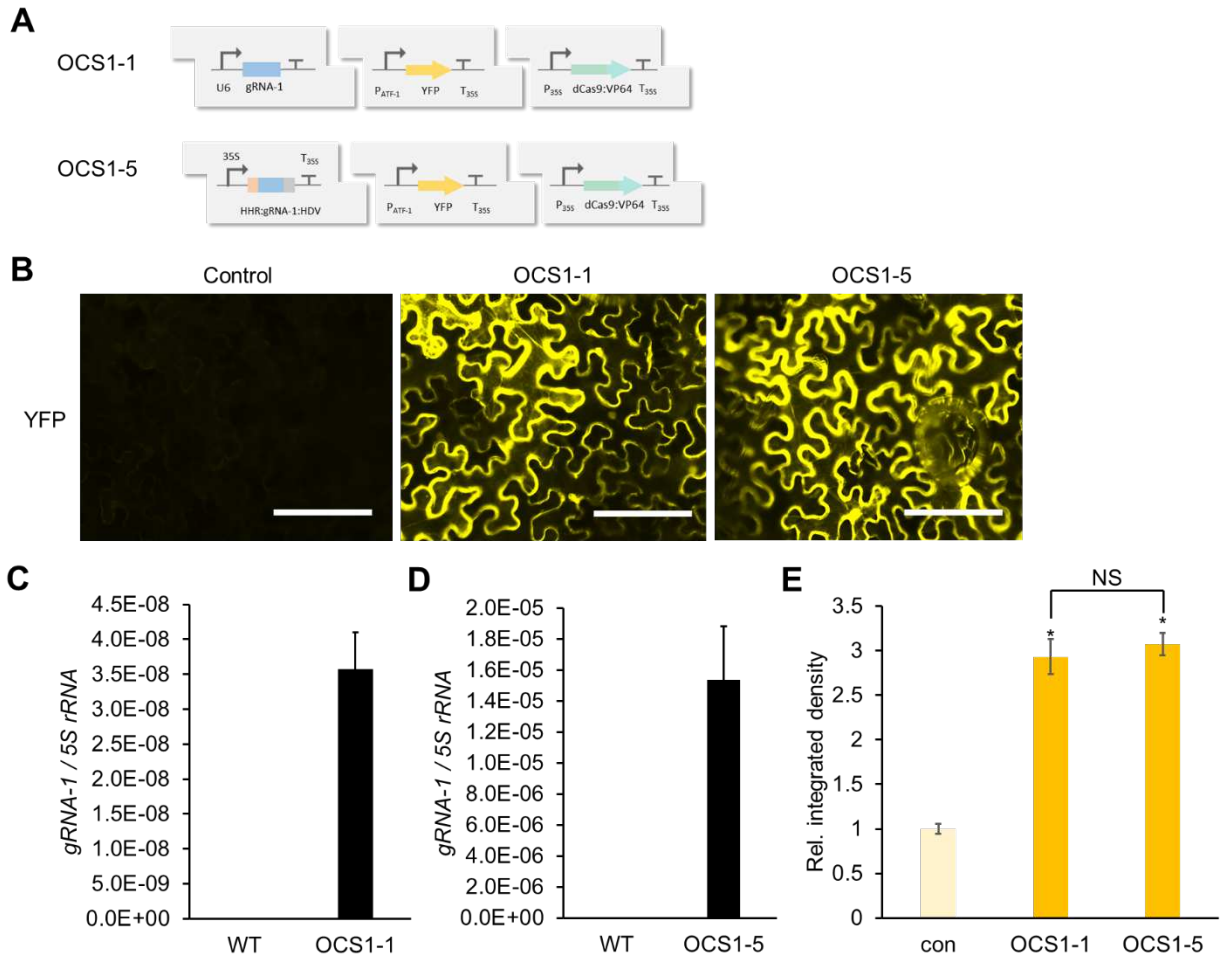
712 construct.

A**B****C**

714 **Figure 3. Characterization of activity of synthetic pATF promoters. A.** Circuit design
715 of dCas9 based artificial transcription factor-controlled activation of synthetic promoters
716 (pATFs). Specific *gRNAs* are produced by U6 promoter while the expression of the
717 dCas9-VP64 is under the control of the 35S promoter. Reporter genes are under the
718 control of the synthetic promoter (3 repeats of the *gRNA* followed by minimal 35S
719 promoter to the artificial promoter (*gRNA* binding site) upstream of a specific fluorescence
720 reporter. **B.** Fluorescence microscope image showing Agrobacterium mediated transient
721 expression of YFP, BFP and RFP into *Nicotiana benthamiana* leaves with dCas9-VP64
722 (bottom panels) and without dCas9-VP64 (upper panels) using three different *gRNAs*.
723 Images were captured using the appropriate filter (Materials and Methods) at same
724 exposure. **C.** Relative integrated density of each fluorescence signal (shown in panel B).
725 Integrated density was measured using image J software and normalized to that of the
726 control (con; - dCAS9-VP64). Error bars: S.D. (n=3, independent replicates). Asterisks
727 indicate statistical significance in a student t-test (P<0.05).



728
 729 **Figure 4. Evaluation of OCS reporter gene expression in transgenic *Arabidopsis***
 730 **plants. A.** Image showing Kanamycin selection of the transgenic *Arabidopsis* seedlings
 731 on MS media. Seedlings highlighted in the red circle have successfully incorporated OCS
 732 circuit. Transformation efficiency is within reasonable ranges (~1%) determined by a
 733 simple evaluation of the identified seedlings. **B.** Fluorescence microscope image of
 734 *Arabidopsis* transgenic T₁ plants containing the constitutive expression of YFP under the
 735 OCS control (OCS 1-1). Scale bar: 50 μm **C.** Image showing Kanamycin selection of the
 736 transgenic *Arabidopsis* seedlings on MS media using luminescence reporter (OCS4-1)
 737 taken using the NightOwl (Methods). **D.** Image of a T₁ *Arabidopsis* plant containing OCS4-
 738 1 at the rosette stage after spraying the luciferin (Methods) containing OCS4-1. This
 739 image, taken at the rosette stage using NightOwl after luciferin spray, shows that the
 740 luciferase expression is active throughout the adult plant. A non-transgenic plant on the
 741 left was used as a negative control in the luminescence reporter assay.



742

743

744

745

746

747

748

749

750

751

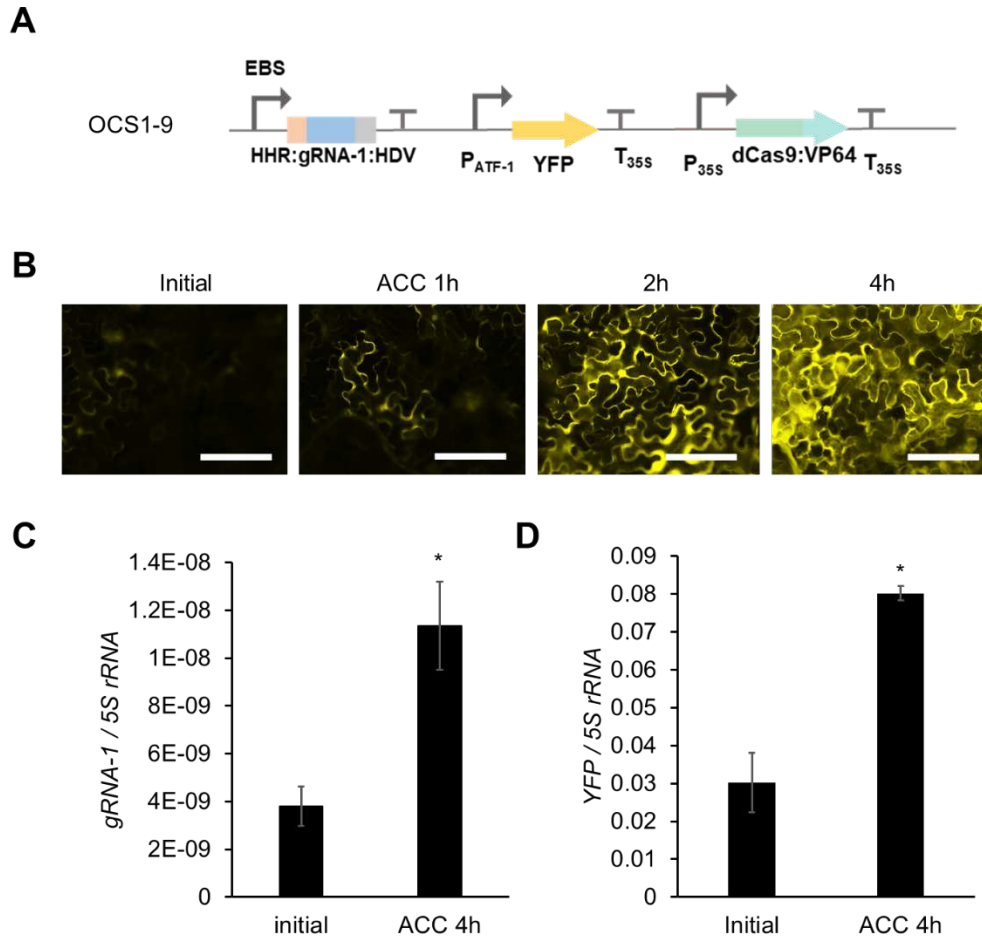
752

753

754

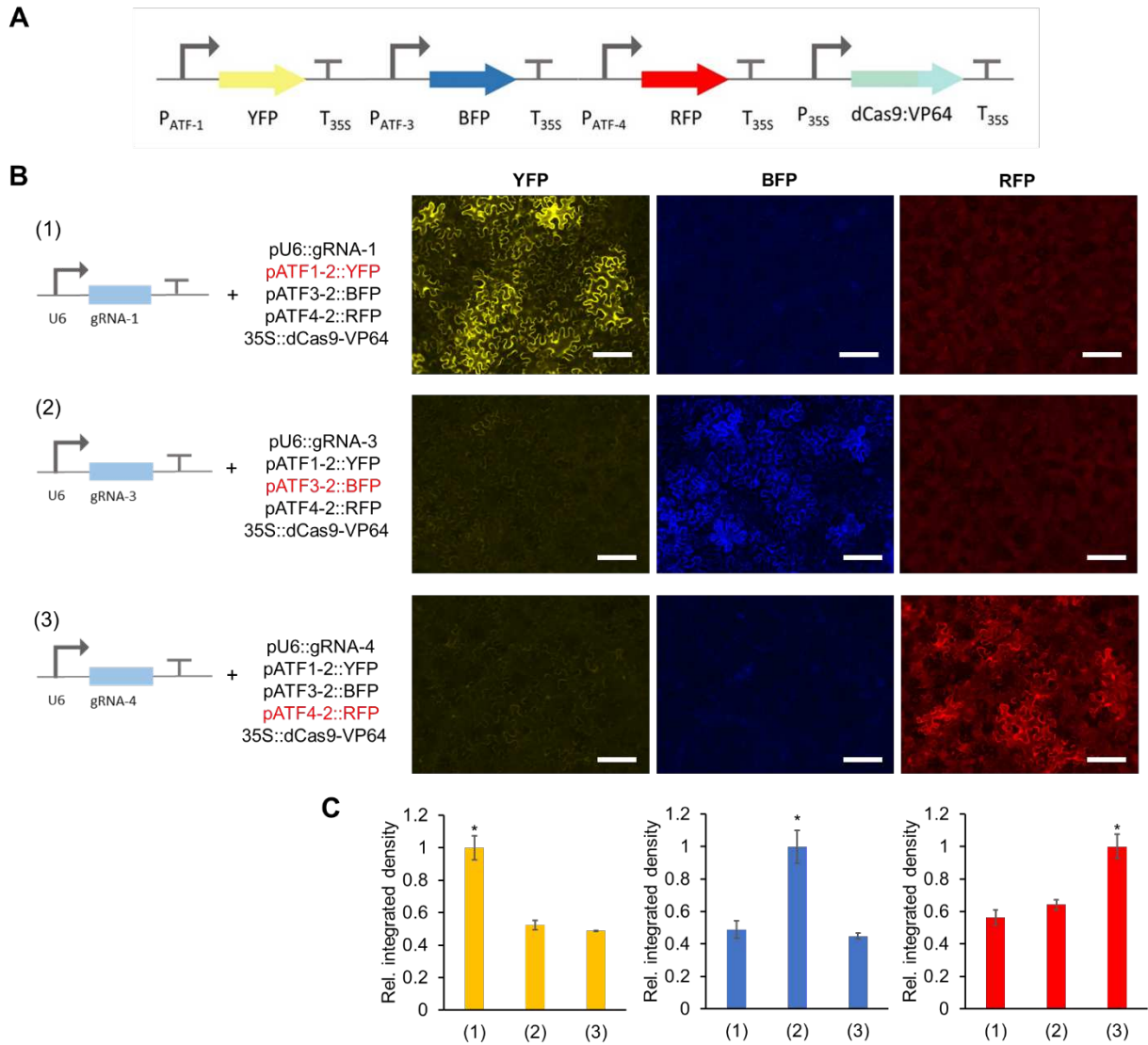
755

Figure 5. Design and characterization of gRNA expression modules under the control of Pol II promoters. **A.** OCS1-1 circuit generates RNA using U6 (Pol III) promoter while OCS1-5 circuit generates gRNA using 35S (Pol II) promoter flanked by self-cleaving ribozymes – HammerHead (HHR) and Hepatitis Delta Virus (HDV). **B.** Fluorescence microscope images showing *Agrobacterium* mediated transient expression of OCS constructs with two modalities of gRNA expression (OCS1-1 and OCS1-5). Control images were taken without dCAS9-VP64 expression. Scale bars: 200 μ m **C** and **D.** Quantification of the *gRNA-1* expression in OCS constructs (OCS 1-1 (C) and OCS 1-5 (D)) using qPCR relative to *5S rRNA*. Error bars : S.D. (n=3, independent replicates) **E.** Relative integrated density of each fluorescence signal (shown in panel B). Integrated density was measured using image J software and normalized to that of the control (con; - dCas9-VP64). Error bars: S.D. (n=3, independent replicates). Asterisks indicate statistical significance in a student t-test ($P < 0.05$). NS: not significant.



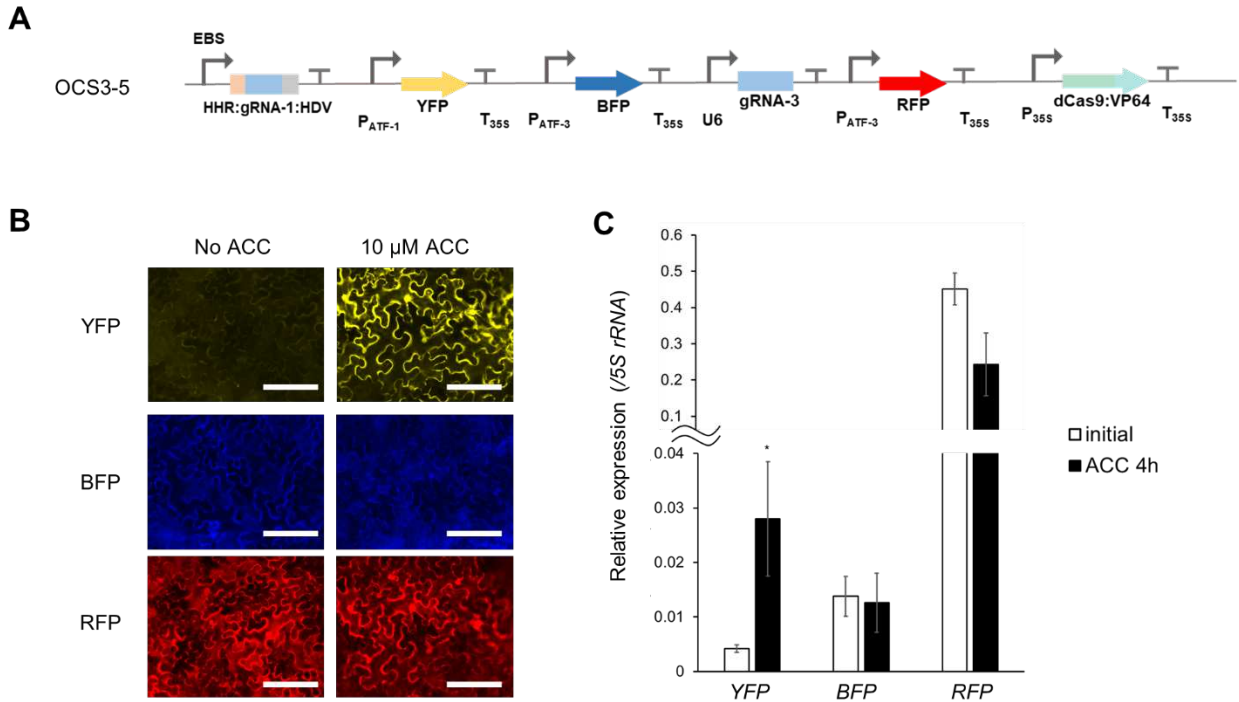
756

757 **Figure 6. Characterization of an ethylene inducible orthogonal control system. A.**
 758 OCS1-9 circuit (*gRNA-1* is expressed by ethylene inducible EBS promoter) **B.** Time
 759 course fluorescence microscope images showing *Agrobacterium* mediated transient
 760 expression of OCS1-9 in *Nicotiana benthamiana* leaves after induction with 10 μ M ACC.
 761 Scale bars: 200 μ m **C and D.** qPCR quantification of *gRNA-1* (C) and *YFP* (D) expression
 762 before and after induction with ACC, where both show similar levels of induction
 763 demonstrating that the relative change in *gRNA-1* expression (ethylene induction) results
 764 in the differential activation from the pATF-1 promoter. Error bars: S.D. (n=3, independent
 765 replicates), Asterisks indicate statistical significance in a student t-test (P<0.05).



766

767 **Figure 7. Degree of orthogonality of synthetic promoters.** **A.** OCS circuit containing
 768 all three synthetic promoters (pATF-1, pATF-3 and pATF-4) driving three different reporter
 769 genes namely YFP, BFP and RFP respectively with a single gRNA expressed one at a
 770 time under the control of U6 promoter. **B.** Fluorescence microscope images showing
 771 *Agrobacterium* mediated transient expression of OCS constructs in *Nicotiana*
 772 *benthamiana* leaves. Scale bars: 200 μ m **C.** As observed from the fluorescence images,
 773 only the specific gRNA:pATF pair is active, thus demonstrating that the synthetic
 774 promoters are mutually orthogonal. Relative integrated density of each fluorescence signal
 775 (shown in panel B). Integrated density was measured by image J software and normalized
 776 to the highest value. Error bars: S.D. (n=3, independent replicates). Asterisks indicate
 777 statistical significance in a student t-test ($P < 0.05$).



778

779

780

781

782

783

784

785

786

787

788

Figure 8. Design and characterization of a ratiometric circuit. A. OSC3-5 contains YFP which is inducible by ACC (pATF-1), while BFP and RFP are constitutively expressed under the control of pATF-3 via the constitutive expression of gRNA-3. **B.** Fluorescence microscope images showing *Agrobacterium* mediated transient expression of the ratiometric OCS construct (OCS3-5) in *Nicotiana benthamiana* leaves with or without 10 μ M ACC. Scale bars: 200 μ m **C.** qPCR quantification of YFP, BFP and RFP shows that YFP is induced after the treatment with ACC while the expression of BFP and RFP remains unchanged before or after ACC induction. Error bars: S.D. (n=4, independent replicates). An asterisk indicates statistical significance in a student t-test (P < 0.05).

Supplementary Files

This is a list of supplementary files associated with this preprint. Click to download.

- [OCSplantsuppV2.pdf](#)
- [OCS11.gb](#)
- [OCS15.gb](#)
- [OCS19.gb](#)
- [OCS35.gb](#)
- [OCS41.gb](#)
- [pAPT.Ex.KanR.gb](#)